JACS
JOURNAL OF THE AMERICAN CHEMICAL SOCIETY

Communication

pubs.acs.org/JACS

Metal–Organic Framework Threaded with Aminated Polymer Formed *in Situ* for Fast and Reversible Ion Exchange

Liang Gao, Chi-Ying Vanessa Li,* Kwong-Yu Chan,* and Zhe-Ning Chen

Department of Chemistry, The University of Hong Kong, Pokfulam Road, Pokfulam, Hong Kong

Supporting Information

ABSTRACT: A porous metal–organic framework composite with flexible anion-exchange polymers threaded within the host cavity demonstrates very fast and reversible ion-exchange activity. Polyvinyl benzyl trimethylammonium hydroxide (PVBTAH) caged in ZIF-8 is synthesized in steps of chloro-monomer impregnation, *in situ* polymerization, amination, and alkaline ion exchange. The synthesized non-cross-linked PVBTAH∼ZIF-8 material exhibits superior ion-exchange kinetics compared to conventional ion-exchange resins.

Porous coordinated polymers[1a] (PCP), or metal–organic frameworks[1b] (MOF), have rapidly grown in varieties and developed collectively into a new class of nanoporous materials, as reviewed recently.[2] Apart from the high surface area, high porosity, and diverse functionality, MOF has combined the advantages of a ceramic matrix, having a regular pore structure, and those of a polymer with elasticity in the interconnecting organic linkers. Applications in catalysis,[3] conductivity,[4] adsorption, and separation[5] have been convincingly demonstrated. Application of MOF's inherent advantages of high porosity, controlled swelling, and high selectivity to ion-exchange applications, however, has been seldom reported.[6] Conventional ion-exchange materials have many shortcomings such as irregular pore structure in polymeric resin and with ion-exchange sites inaccessible to ions.[7,8] Attempts have been made to have a structure with a hydrophobic core and external hydrophilic functional groups.[7] On the other hand, molecular sieves and ceramic materials have slow ion-exchange behavior. Although hybrid material of ion-exchange polymer confined in ordered mesoporous silica materials has been proposed, there is still significant diffusion resistance in the inflexible porous structure of ordered mesoporous silica.[9] In addition, silica materials can degrade in solution with pH > 7.5.[10]

In the anion-exchangeable MOFs reported,[6] a charged metal ion serves as the anchor of the MOF framework and is multicoordinated by the organic linkers. As opposed to a fixed charge on a flexible polymer chain, the charge on the metal is less accessible and can only be positive. Anion trapping and selection behavior are displayed, but, as mirrored in behavior of charged zeolite, these materials are not stable in pH >13. The types of exchangeable anions are also limited. In a different context, Sadakiyo et al.[11] recently reported an organic salt, alkylammonium hydroxide caged in ZIF-8, with ionic conductivity measured. The salt caged in MOF has freely exchangeable OH^- anions but can only function in dry conditions to avoid leaching in aqueous solution, thus limiting applicability for aqueous ion exchange.

Kitagawa and coworkers[12] reported polymers confined within MOFs by *in situ* polymerization of impregnated monomers. Examples include polystyrene, poly(ethylene glycol), and polyvinyl carbazole into MOFs which include La(1,3,5-benzenetrisbenzoate) and $[M_2(L)_2ted]$ (L = dicarboxylate; ted = triethylenediamine; M = Cu or Zn). The polymers within MOFs have nanoconfinement behavior with structural, physical, and chemical properties deviated from those of the bulk.

Inspired by their works, we extend the concept of "polymerization in MOF" to include polymers amenable to further functionalization to provide ion-exchangeable sites. We demonstrate for the first time the amination of polymer caged in MOF with the desirable ion-exchange functionality. This ion-exchange polymer threaded in the MOF pore network is sufficiently interlocked to prevent entrainment in aqueous solution, while the free and flexible polymer chain has its charged sites in full contact with aqueous solution, thus facilitating very fast ion-exchange behavior.

In principle, this approach can be applied to cation exchange polymers including sulfonic and phosphoric types,[8] and into different MOFs which are stable in a wide range of pH as those listed in Table S2. We verify here the concept of "ion-exchange polymer threaded in MOF" by synthesizing poly vinyl benzyl trimethylammonium hydroxide (PVBTAH), a strongly basic polymer, into ZIF-8, a MOF that can be stable in 8 M NaOH at 100 °C.[13]

The synthesis of the PVBTAH∼ZIF-8 is outlined in Figure 1. Vinyl benzyl chloride (VBC) monomers are impregnated into the nanopores of ZIF-8. By thermal activation, *in situ* radical polymerization of monomer units across nanocages occurs and leads to poly vinyl benzyl chloride (PVBC) threaded and interknitted within the MOF pore network. Subsequent amination of PVBC∼ZIF-8 yields poly vinyl benzyl trimethylammonium chloride (PVBTAC). The free anionic chloride group formed, as a type I strong basic ion-exchange resin,[8] allows further exchange with OH^- anion to form poly vinyl benzyl trimethylammonium hydroxide (PVBTAH) in ZIF-8. The absence of a cross-linking agent in the polymerization ensures linear chains formed in the final structure.

The unique features of the PVBTAH∼ZIF-8 composite structure are highlighted in Figure 2a and compared with the structure of a conventional polymeric ion-exchange resin in Figure 2b. Due to confinement of the monomers and the absence

Received: February 25, 2014
Published: May 6, 2014

   dx.doi.org/10.1021/ja501958u | J. Am. Chem. Soc. 2014, 136, 7209–7212

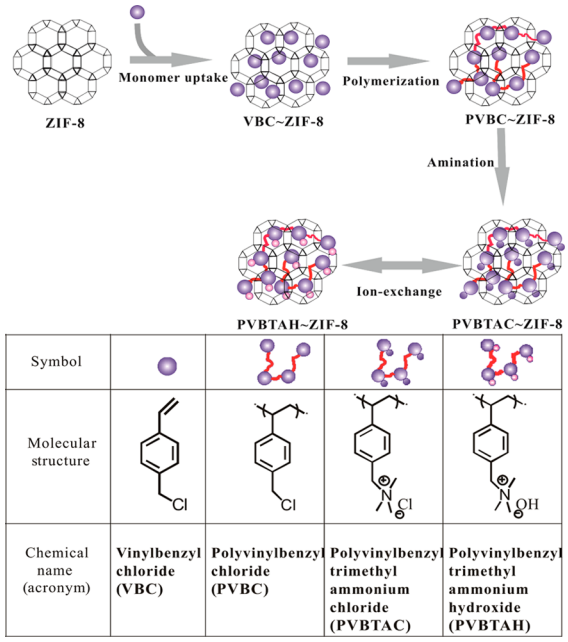

Figure 1. Synthesis of ion-exchange polymer (PVBTAH) threaded within the porous network of ZIF-8.

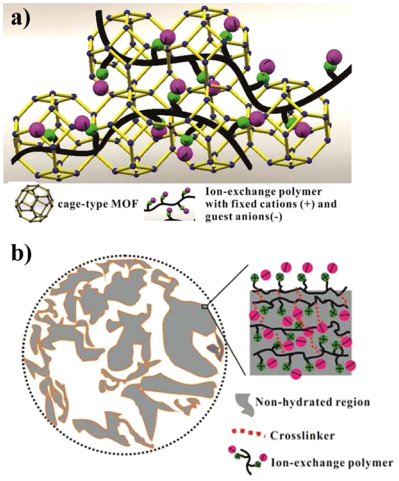

Figure 2. Schematic illustration of the structures of ion-exchange materials: (a) PVBTAH~ZIF-8 and (b) microscopic view of a standard ion-exchange resin with random pore distribution, e.g., Amberlyst-A26, with majority of active sites hidden inside the nonhydrated regions of the bead.

of cross-linking agent, the *in situ* synthesized PVBC and the subsequently derived PVBTAC and PVBTAH are all linear. The polymer chains are segregated by the ordered MOF structure without entanglement. Thus, they can be in full contact with a solvent that enters the open framework. The fully solvated polymers, on the other hand, are trapped within the MOF framework and prevented from entrainment. This composite material has an overall heterogeneous matrix but contains local homogeneous active domains. Accessibility to the bulk solution and enhanced diffusion is an important feature as discussed in ion-exchange polymer coated fibers and silica.[14] On the other hand, the charged sites of a conventional polymeric ion-exchange material are unevenly distributed inside the resin, composed of cross-linked chains and a highly irregular pore structure with limited hydrated domains (Figure 2b). The synthesized PVBTAH~ZIF-8 and intermediates PVBTAC~ZIF-8 and PVBC~ZIF-8 are characterized in detail to confirm the features of Figure 2a. Selected properties of ZIF-8 and PVBTAH~ZIF-8 composite are summarized in Table 1 and compared with those of a commercial Amberlyst-A26 anion exchange polymer.

The synthesized polymers~ZIF-8 materials are micrometer scale particles (Figure S1). Uniform distribution of the polymer in the porous MOF is indicated by energy dispersive X-ray fluorescence (EDX) mapping of Zn and Cl in PVBC~ZIF-8 (Figure S2). Other experimental reports also demonstrated the ease of VBC monomers penetration into ZIF-8.[15] From theoretical analyses using lattice of ZIF-8 (Figure S4), a VBC molecule at liquid state is favorably attracted into ZIF-8 with an energy change of −3.7 kcal/mol (Figure S5). Due to its small size, the penetration barrier is not high at 18.8 kcal/mol. The aminated molecule, VBTAC, in a typical simulated equilibrium configuration resides off-center in a cavity of ZIF-8, as shown in Figure S6.

The ZIF-8 MOF structures in the various synthesized composites remain intact, as shown by almost identical X-ray diffraction spectra of the PVBC~ZIF-8, PVBTAC~ZIF-8, PVBTAH~ZIF-8, and the parent ZIF-8 (Figure S7) as well as the uniform Zn distribution in the EDX mapping of PVBC~ZIF-8 (Figure S2). The slight shift in the XRD peaks corresponds to a very small expansion of PVBC~ZIF-8 lattice (17.097 Å) from the parent ZIF-8 lattice (17.019 Å) (Figure S7b), whereas a control sample of physically mixed ZIF-8 and PVBC shows no shifts in the XRD pattern. Similar lattice expansions have been observed in other MOF caged polymer nanocomposites.[12a]

After removing the host ZIF-8 structure by acid wash, the number-averaged molecular weight (M_n) of PVBC is determined

Table 1. Structural and Ion-Exchange Properties of ZIF-8, PVBTAH~ZIF-8 composite, and Amberlyst-A26

sample	S_{BET} (m^2/g)[a]	V_p (mL/g)[b]	D (g/mL)[c]	pore width (nm)[d]	ion-exchange capacity (IEC) by wt (meq/g)	ion-exchange capacity (IEC) by vol (meq/mL)	Hoffmann degradation temperature (°C)[e]
ZIF-8	1045	0.49	0.35	0.66	0	0	–
PVBTAH~ZIF-8	600	0.26	~1.06[f]	0.45	~0.6[g]	~0.636[I]	~123
Amberlyst-A26 ion-exchange resin	30	0.3	0.64	irregular macropore	4.4[h]	0.8[j]	~96

[a]Determined by N_2 sorption isothermal at 77K. [b]Determined by t-plot method; For Amberlyst-A26, value is macropore volume from Sigma-Aldrich. [c]Density measured by a 5 mL pycnometer using cyclohexane (density 0.779 g/mL at 20 °C). [d]Determined by HK model of slit pore which gives correct value of 0.5 nm for a zeolite 5A standard; the alternative DFT analyses based on cylindrical pore shape gives 1.2 nm for ZIF-8 and 1.1 nm for PVBTAH~ZIF-8. [e]From TPD-MS results of Figure S16. [f]This value is obtained without complete drying. [g]Based on the total weight of PVBTAH~ZIF-8. [h]Data from Sigma-Aldrich for dry resin in Cl form. [I]Converted from measure density as noted in (*f*). [j]Data from Sigma-Aldrich for a wet resin.

dx.doi.org/10.1021/ja501958u | *J. Am. Chem. Soc.* 2014, 136, 7209−7212

by GPC to be 1843 (Figure S8), corresponding to ~12 monomer units.

ZIF-8 and PVBC~ZIF-8 are both hydrophobic, whereas PVBTAC~ZIF-8 and PVBTAH~ZIF-8 become strongly hydrophilic with the ionic groups added. Figure S9 shows their partitioning between octane and water phases. After amination, PVBTAC~ZIF-8 becomes miscible with water but not leached out. The synthesized polymers must have resided inside the cavities of ZIF-8. Loose PVBTAC or PVBTAH strings adhered on particle surfaces will be washed away during synthesis and ion-exchange steps.

Successful amination to PVBTAC~ZIF-8 is confirmed by FTIR with the appearance of a quaternary ammonium peak at ~3024 cm^{-1} and accompanied by disappearance of the C−Cl peak (Figure S10). When the ZIF-8 host is etched away by HCl, the released PVBTAC has proton NMR peaks matching well with those of a bulk PVBTAC (Figure S11). The peaks at ~3 and ~6−8 ppm correspond to the quaternary ammonium group and the aromatic ring of PVBTAC,[16] respectively. The line-width broadening at 6−8 ppm implies both samples have the polymer chain conformation. To enhance the ion exchange character, PVBTAC~ZIF-8 is converted to hydroxide form by alkaline treatment. Successful conversion is indicated by the disappearance of Cl peaks in the EDX spectrum (Figure S3).

N_2 physisorption analysis (Figure S12) indicates a significant decrease in Brunauer−Emmett−Teller (BET) surface area from 1045 to 600 m^2/g and pore volume from 0.49 to 0.26 mL/g of the ZIF-8 after incorporation of PVBTAH. This decrease in pore volume is accompanied by a slight decrease in pore size of the ZIF-8, as analyzed by the Horvath−Kawazoe (HK) model of slit-shape micropores (Figure S13).

A unit cell of ZIF-8 has a cavity surrounded by 12 windows 0.49−0.80 nm wide and interior sufficient to host a 1.16 nm diameter sphere.[17] To understand the small change in pore size in contrast to the large change in pore volume, equilibrium configuration of a VBTAC molecule inside ZIF-8 is computed and shown in Figure S6. A VBTAC monomer occupies a good part of the cavity in ZIF-8 but stays near the side wall, leaving most of the channel unobstructed, as viewed down a channel in Figure S6. The 0.45 nm pore size determined by HK model and the channel of ZIF-8 in Figure S6 are both sufficiently large to accommodate common ions. Upon polymerization, a pair of adjacent monomer units would be connected through one of the windows. Other windows can allow free entrance of ions and solvent. Polymerization must have occurred across different adjacent cavities. TGA of PVBC~ZIF-8 shows 13% additional weight loss compared with neat ZIF-8 (Figure S14b). This is in agreement with the EDX result of 14 wt % PVBC loading (Figure S2). Nanoconfinement of one unit of PVBC per cavity, the linearity of the polymer chains segregated by the ZIF-8 lattice is supported by absence of a glass transition temperature (T_g) for the PVBC~ZIF-8 material. In contrast, bulk PVBC synthesized under identical conditions or a physical blend of bulk ZIF-8 and PVBC all have a T_g of 105 °C (Figure S15). Thus, there is no observable presence of PVBC outside the porous regions of ZIF-8, which otherwise will lead to an observable T_g.

Strongly basic ion-exchange polymers with OH form undergo Hoffmann degradation,[8] such as the Amberlyst-A26 with a degradation temperature of 96 °C as observed in TPD-MS experiment (Figure S16a). PVBTAH~ZIF-8, however, does not degrade until a higher temperature of 123 °C (Figure S16b). This is in agreement with the TGA result of PVBTAH~ZIF-8 (Figure S14c). No degradation is observed in PVBTAC~ZIF-8 which has chloride instead of OH^- (Figure S16c). The superior thermal stability of PVBTAH~ZIF-8 compared to Amberlyst-A26 can be rationalized by the absence of cross-linking, resulting in enhanced polymer flexibility. Improved thermal stability by increased degree of freedom, including elasticity in non-cross-linked polymer, has been suggested.[8]

Isolation of the polymer chains from each other lead to increase in free volume. The bulk density of PVBC is 1.16 g/cm^3 and corresponds to a specific volume of 0.86 cm^3/g. The apparent specific volume of PVBC in ZIF-8 is estimated to be >1.3 cm^3/g by micropore volume analyses (Table S2). This significant increase in free volume, as illustrated by the isolated polymer chain in Figure 2a will lead to excellent functionality in ion-exchange. The ion-exchange performance of the PVBTAH~ZIF-8 material and Amberlyst-A26 is tested in nitrate and gold cyanide solutions. Concentrations of NO_3^- solutions with ion-exchange materials immersed are monitored by UV−vis spectroscopy (Figure S17). Although the long time nitrate removal is similar in both cases (Figure S18), the initial kinetics is markedly different. There is a rapid decrease of >50% in the nitrate peak within 1 min, compared to >60 min required for Amberlyst-A26 resin. Most likely, the fast ion exchange is provided by the highly porous ZIF-8, possessing enhanced adsorption behavior compared to its counterpart.

Ability of the PVBTAH~ZIF-8 material to scavenge precious metal at trace concentrations is evaluated by its interaction with ppm level gold cyanide solution, which represents a typical precious metal electroplating waste water needing treatment for economic and environmental incentives.[7] After immersing in 15 mg/L gold solution, the PVBTAH~ZIF-8 material is analyzed to have a FTIR peak at 2142 cm^{-2}, corresponding to the CN bond (Figure S19), thus confirming the loading of gold cyanide anion by ion exchange. Such CN peak is not observed for neat ZIF-8 soaked in the same gold cyanide solution, ruling out the possibility of loading by adsorption. Integrity of the MOF structure is indicated by identical XRD patterns of the gold cyanide loaded PVBTAH~ZIF-8 and that of neat ZIF-8 (Figure S7c). Shown in Figure 3, the extraction rate by PVBTAH~ZIF-8

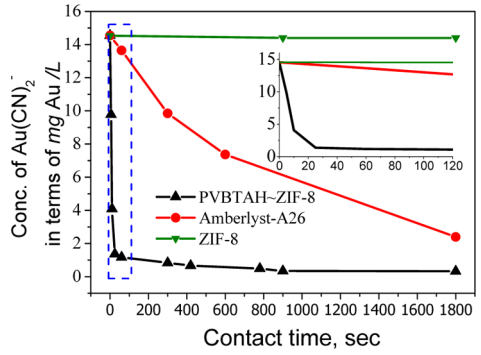

Figure 3. $Au(CN)_2^-$ concentration, expressed in mg gold per liter, after immersing equal masses of PVBTAH~ZIF-8 and Amberlyst-A26 in $KAu(CN)_2$ solution. Inset: enlarged profiles of the first 120 s.

is much higher than that of Amberlyst-A26. In 25 s, > 90% gold cyanide anion has been extracted, compared to 7% extraction by Amberlyst-A26. Equilibrium adsorption is established after 5 min with PVTAH~ZIF-8, compared to 30 min for Amberlyst-A26.

The ion-exchange experiments are performed on the basis of equal weights of PVBTAH~ZIF-8 and Amberlyst-A26. Though, the latter has a higher capacity based on dry weight, capacity

dx.doi.org/10.1021/ja501958u | J. Am. Chem. Soc. 2014, 136, 7209−7212

based on wet volume is similar, as shown in Table 1. The ion-exchange sites in PVBTAH∼ZIF-8 are utilized more effectively and can be attributed to the ideal features of the structure shown in Figure 2, with high surface area and large free volume. On the other hand, the ion-exchange sites of commercial resins are embedded in non-uniform macro-reticular porous structure and subject to serious mass-transfer limitations. The fast ion-exchange activity can be demonstrated in the reverse direction with $Au(CN)_2^-$ ion eluting from the $Au(CN)_2^-$ loaded PVBTAH∼ZIF-8, thus enabling robust and reversible use of the material. The $Au(CN)_2^-$ loaded PVBTAH∼ZIF-8 sample is stripped of $Au(CN)_2^-$ by immersion in ethanolic solution of NaOH. Recovery of $Au(CN)_2^-$ from the $Au(CN)_2^-$ loaded PVBTAH∼ZIF-8 sample can be completed in the first minute (Figure S20). Repeated cycles of extraction-reverse extraction show robust and reversible ion-exchange activity of PVBTAH∼-ZIF-8. On the other hand, the Amberlyst-A26 degraded in a few cycles due to mechanical deformation.

Although Amberlyst-A26 have a high exchange capacity on dry weight basis, its capacity is only 0.8 meq/mL on a wet basis, due to significant swelling. This is comparable to the value of PVBTAH∼ZIF-8. Rate of exchange is probably a more important parameter since typical commercial resins need orders of hours to fully realize its capacity. Kinetics also impact on continuous process and effective reversible use of ion exchange material which is of increase priority for sustainability.

In conclusion, we report a strongly basic ion-exchange polymer threaded in MOF with high surface area, high porosity, and facile accessibility. Amination of a polymer caged in MOF is reported for the first time. Superior performance of a strongly basic ion-exchange polymer, PVBTAH, threaded in ZIF-8 is demonstrated by fast, complete, reversible, and robust extraction of gold at trace concentrations. This approach of confining ion-exchange polymers within MOFs may be extended to some MOFs with good chemical stability in acid/base solution (see Table S2). Certain anions, like bidentate carboxylates or tridentate carboxylates, can replace the framework-forming ligand via a "post-synthetic exchange" process, and applications in their salt solutions should thus be avoided. The high surface area and easy accessibility of guest species enable the proposed ion-exchange polymer∼MOF composite to function in gas phase or non-polar environment, in which conventional ion-exchange materials show poor performance owing to inaccessibility of their internally embedded active sites.

■ ASSOCIATED CONTENT

Supporting Information

Procedures and calculations. This material is available free of charge via the Internet at http://pubs.acs.org/.

■ AUTHOR INFORMATION

Corresponding Authors

hrsccky@hku.hk
cyvli@hku.hk

Notes

The authors declare no competing financial interest.

■ ACKNOWLEDGMENTS

We acknowledge financial supports from Research Grants Council of Hong Kong (GRF HKU 700210P), Strategic Research Theme on Clean Energy, and University Development Fund for Initiative for Clean Energy and Environment. Mr. Frankie Chan of EMU provided technical assistance in electron microscopy. GPC experiments were performed with kind assistance of Miss Haiting Shi and Prof. W.K. Chan.

■ REFERENCES

(1) (a) Kindo, M.; Yoshitomi, T.; Matsuzaka, H.; Kitagawa, S.; Seki, K. *Angew. Chem., Int. Ed.* **1997**, *36*, 1725. (b) Li, H.; Eddaoudi, M.; O'Keeffe, M.; Yaghi, O. M. *Nature* **1999**, *402*, 276.

(2) (a) Kitagawa, S.; Kitaura, R.; Noro, S. I. *Angew. Chem., Int. Ed.* **2004**, *43*, 2334. (b) Furukawa, H.; Cordova, K. E.; O'Keeffe, M.; Yaghi, O. M. *Science* **2013**, *341*, 1230444. (c) Ferey, G. *Chem. Soc. Rev.* **2008**, *37*, 191. (d) Lee, J.; Farha, O. K.; Roberts, J.; Scheidt, K. A.; Nguyen, S. T.; Hupp, J. T. *Chem. Soc. Rev.* **2009**, *38*, 1450. (e) Murray, L. J.; Dincă, M.; Long, J. R. *Chem. Soc. Rev.* **2009**, *38*, 1294. (f) Jiang, H.; Xu, Q. *Chem. Commun.* **2011**, *47*, 3351.

(3) (a) Jiang, H. L.; Liu, B.; Akita, T.; Haruta, M.; Sakurai, H.; Xu, Q. *J. Am. Chem. Soc.* **2009**, *131*, 11302. (b) Wang, C.; deKrafft, K. E.; Lin, W. *J. Am. Chem. Soc.* **2012**, *134*, 7211.

(4) (a) Wiers, B. M.; Foo, M. L.; Balsara, N. P.; Long, J. R. *J. Am. Chem. Soc.* **2011**, *133*, 14522. (b) Hurd, J. A.; Vaidhyanathan, R.; Thangadurai, V.; Ratcliffe, C. I.; Moudrakovski, I. L.; Shimizu, G. K. H. *Nat. Chem.* **2009**, *1*, 705. (c) Bureekaew, S.; Horike, S.; Higuchi, M.; Mizuno, M.; Kawamura, T.; Tanaka, D.; Yanai, N.; Kitagawa, S. *Nat. Mater.* **2009**, *8*, 831.

(5) (a) Herm, Z. R.; Wiers, B. M.; Mason, J. A.; van Baten, J. M.; Hudson, M. R.; Zajdel, P.; Brown, C. M.; Masciocchi, N.; Krishna, R.; Long, J. R. *Science* **2013**, *340*, 960. (b) Mason, J. A.; Veenstra, M.; Long, J. R. *Chem. Sci.* **2014**, *5*, 32. (c) Rosi, N. L.; Eddaoudi, M.; Vodak, D. T.; Eckert, J.; O'Keeffe, M.; Yaghi, O. M. *Science* **2003**, *300*, 1127−1129.

(6) (a) Zhao, X.; Bu, X.; Wu, T.; Zheng, S. T.; Wang, L.; Feng, P. *Nat. Commun.* **2013**, *4*, 2344. (b) Fei, H.; Rogow, D. L.; Oliver, S. R. J. *J. Am. Chem. Soc.* **2010**, *132*, 7202. (c) Fei, H.; Pham, C. H.; Oliver, S. R. J. *J. Am. Chem. Soc.* **2012**, *134*, 10729. (d) Genna, D. T.; Wong-Foy, A. G.; Matzger, A. J.; Sanford, M. S. *J. Am. Chem. Soc.* **2013**, *135*, 10585.

(7) Lam, Y. L.; Yang, D.; Chan, C. Y.; Chan, K. Y.; Toy, P. H. *Ind. Eng. Chem. Res.* **2009**, *48*, 4975.

(8) Harland,C. E. *Ion-exchange: Theory and Practicle*, 2nd ed.;, Royal Society of Chemistry: London,1994.

(9) Choi, M.; Kleitz, F.; Liu, D.; Lee, H. Y.; Ahn, W. S.; Ryoo, R. *J. Am. Chem. Soc.* **2005**, *127*, 1924.

(10) Law, B.; Chan, P. F. *J. Chromatogr.* **1989**, *461*, 267.

(11) Sadakiyo, M.; Kasai, H.; Kato, K.; Takata, M.; Yamauchi, M. *J. Am. Chem. Soc.* **2014**, *136*, 1702.

(12) (a) Uemura, T.; Hiramatsu, D.; Kubota, Y.; Takata, M.; Kitagawa, S. *Angew. Chem., Int. Ed.* **2007**, *119*, 5075. (b) Distefano, G.; Comotti, A.; Bracco, S.; Beretta, M.; Sozzani, P. *Angew. Chem., Int. Ed.* **2012**, *51*, 9258. (c) Uemura, T.; Kitagawa, K.; Horike, S.; Kawamura, T.; Kitagawa, S.; Mizuno, M.; Endo, K. *Chem. Commun.* **2005**, 5968. (d) Distefano, G.; Suzuki, H.; Tsujimoto, M.; Isoda, S.; Bracco, S.; Comotti, A.; Sozzani, P.; Uemura, T.; Kitagawa, S. *Nat. Chem.* **2013**, *5*, 335. (e) Uemura, T.; Yanai, N.; Watanabe, S.; Tanaka, H.; Numaguchi, R.; Miyahara, M. T.; Ohta, Y.; Nagaoka, M.; Kitagawa, S. *Nat. Commun.* **2010**, *1*, 83. (f) Yanai, N.; Uemura, T.; Kitagawa, S. *Chem. Mater.* **2012**, *24*, 4744. (g) Uemura, T.; Uchida, N.; Asano, A.; Saeki, A.; Seki, S.; Tsujimoto, M.; Isoda, S.; Kitagawa, S. *J. Am. Chem. Soc.* **2012**, *134*, 8360.

(13) Park, K. S.; Ni, Z.; Côté, A. P.; Choi, J. Y.; Huang, R.; Uribe-Romo, F. J.; Chae, H. K.; O'Keeffe, M.; Yaghi, O. M. *Proc. Natl. Acad. Sci. U.S.A.* **2006**, *103*, 10186.

(14) (a) Dominguez, L.; Benak, K. R.; Economy, J. *Polym. Adv. Technol.* **2001**, *12*, 197. (b) Harmer, M. A.; Farneth, W. E.; Sun, Q. *J. Am. Chem. Soc.* **1996**, *118*, 7708.

(15) See detail of IV in Supporting Information, pp S4 and S5.

(16) Mitsukami, Y.; Donovan, M. S.; Lowe, A. B.; McCormick, C. L. *Macromolecules* **2001**, *34*, 2248.

(17) Jiang, H. L.; Liu, B.; Lan, Y. Q.; Kuratani, K.; Akita, T.; Shioyama, H.; Zong, F.; Xu, Q. *J. Am. Chem. Soc.* **2011**, *133*, 11854.